Effects of the spacing between two hydrokinetic turbines on the bedforms by numerical simulations

F. Khaled[1,3], S. Guillou[1], Y. Mear[1,2], F. Hadri[3]

Abstract— **Hydrokinetic turbines interact with the dynamics of the sedimentary bottom at small and large scale. Despite the interest that the study of these interactions deserves, little research has been published in the field. In this paper, we investigate by numerical simulation the interaction between modelled hydrokinetic turbines and bed load of sands. The mixture of water and sediment is accounted for by an Eulerian multiphase model developed in the open source platform OpenFOAM. The turbines blades are parameterized by the Blade Element Momentum Theory (BEMT). A good agreement with measurements is obtained in the near wake. The effects of the two different turbine models on the bedload sediment transport are then examined.**

Keywords— **BEMT, Environmental impact, Euler-Euler multiphase, Hydrokinetic turbines, Numerical simulations, Hydrokinetic turbines, OpenFOAM.**

I. INTRODUCTION

Accelerating hydrokinetic renewable energy development towards endurance requires investigating interactions between the hydrokinetic turbine and its surrounding physical environment. Interactions between hydrokinetic turbines (HT) and mobile sediment bed are considered as a critical area of assessment, however limited research studies have been published to address this issue. Hill et al. [1] have shown experimentally that the presence of either single or multiple turbines and the rotation of the blades affect the bed morphology. Musa et al. [2] have investigated experimentally the local effect of streamwise aligned turbines on the bedload, they found as a result that the geomorphic effects are stronger with increasing shear stress due to the presence of the rotors, inducing an alternating scour-deposition phenomenon. Chen et al. [3] have investigated the influence of rotor blade tip clearance (distance between blades and seabed) on the scour rate of pile-supported horizontal axis current turbine. The results suggest that the decrease in tip clearance increases the scour depth, hence more sediment transport. Recently, Khaled et al. [4] have studied the impact of hydrokinetic turbine on erodible sand banks, they showed numerically a significant interaction between the confinement of the turbine and its impact on the near bottom.

In the present issue, we study the impact of two interacting turbines on the near bedform morphology. A modelling framework is derived to predict the significant transport induced by the turbines, such as the Euler-Euler (EE) multiphase model for sediment transport and the Blade Element Method (BEM) to model the forces generated by the turbines, using the open-source platform OpenFOAM and the library SedFoam [5]. A phase of validation is presented for the combined model (EE and BEM) using experimental results of Hill et al. [1]. The present study consists in considering one sediment class, sand of diameter of 0.25 mm, and two horizontal axis turbines with an axial flow direction corresponding to the riverine case. The approach is configured with four different axial inter-turbines distances. The wake distribution behind the second turbine is altered by the wake of the upstream turbine in all configurations.

II. NUMERICAL MODELS

The sediment transport model is based on the Eulerian two-phase flow model for fluid and solid phases [6,7]. The model is incorporated in OpenFOAM as SedFoam by [5]. The turbines are modelled by BEMT and they are represented each by an actuator disk. Details concerning both Euler-Euler model and BEMT model are provided in [4].

The validation of the BEMT model was done by using the experiments of Mycek et al.[8]. The considered flow

The authors acknowledge CRIANN (Centre Régional Informatique et d'Application Numériques de Normandie) co-financed by the Normandy Region, the State and the European Union, for the access to the Computation means and to the Manche Country Concil for their founding

F.Khaled and S.Guillou are at Université de Caen Normandie, LUSAC, EA 4253, 60 rue Max Pol Fouchet, CS 20082, 50130 Cherbourg, France. (e-mail : fatima.khaled@unicaen.fr ; sylvain.guillou@unicaen.fr)

Y.Méar is in INTECHMER/LUSAC, Bd de Collignon, 50110 Tourlaville, France. (e-mail: yann.mear@lecnam.net)

F.Hadri is in LISV, University of Versailles, 78140 Vélizy, France. (ferhat.hadri@uvsq.fr)

Digital Object Identifier: https://doi.org/10.36688/ewtec-2023-554

velocity is $U_\infty = 0.8m/s$ and the hydrokinetic turbine speed corresponds to a Tip Speed Ratio (TSR) of *3.67*. This value corresponds to a speed of rotation of 80 rounds per minute, or approximately *8.38 rad/s*. The disc is of diameter $d = 0.7$ *m* with a thickness of *0.02m* that corresponds to the blade design. The ambient turbulence rate is $I_\infty = 3\%$. Fig. 1 shows the vertical profiles of the axial velocity downstream the turbine. In general, the BEMT results and the measurements have the same trend of evolution near the turbine until *8d* downstream its location. This is in accordance with the theory, so that BEMT is reliable in determining the local effect of the turbine and calculating the local efforts on its blades. Whereas near the turbine, at *1.2d* and *2d*, at the hub position, there is a little difference between the results, this could be due to the fact that the hub geometry and the turbine's support was not taken into consideration in the simulations.

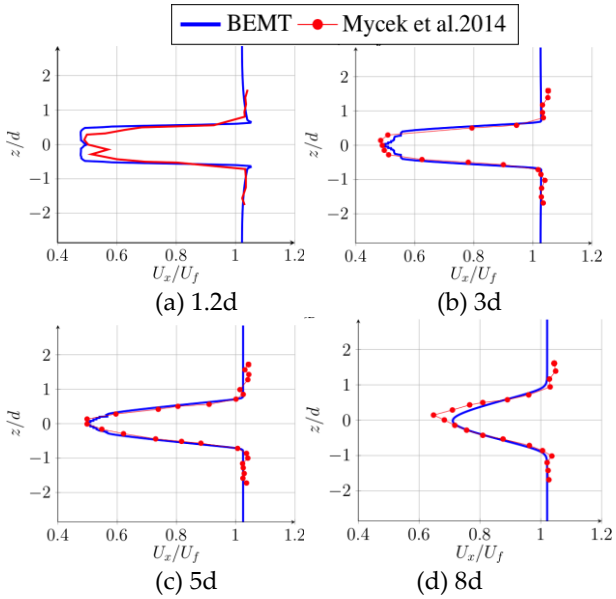

Fig. 1. Vertical profiles of the axial velocity dimensionless by the fluid velocity (U_x/U_∞), downstream the turbine; blue for numerical BEMT results, green for AD results and red for the measurements of [8]

To study the turbines-sediment interactions, the BEMT was coupled with the Euler-Euler model in SedFoam by adding the source terms of BEMT that represents the control volume force [4] to the fluid equations in SedFoam. A validation of the coupled model was made by using the experiments of Hill et al. [1] under clear-water conditions. The simulated channel is 10m long (streamwise direction x), *2.75m* wide (crosswise direction z) and *1.15m* deep (vertical direction y). The rotor diameter of the turbine is $d = 0.5m$. The centre of the rotor is located at *3m* from the inlet and at *0.42m* from the bed surface. The tip speed ratio is *7.1*, while the fluid bulk velocity is *0.56m/s*. The inlet turbulent intensity is of *3%*. The sediment fraction of the sand bed is of *55 %*, with a thickness of *0.15m*, and the sediment diameter is $d_s = 1.8$ *mm*. The granular flow rheology is used to estimate the particular shear stress. The $\mu(I)$ model is used for the solid friction [9]. The viscosity model is the one proposed by Boyer whereas the drag model is the one of Gidaspow [10]. The particle pressure model is the one of Lun [11]. The critical shear stress relating to the parameter is of *1.156 Pa*. The size of time step for the flow simulation is *0.001s*. The entire domain is meshed by *21* million structured hexahedral cells. The computed temporal scour evolution is compared with the measurements of [1] in figure 2 at four spanwise locations ($z = 0$, $z = 0.2d$, $z = 0.4d$ and $z = 0.6d$) *0.1d* downstream of the turbine. The computed bed evolutions are close and show good agreement with the measurements in the near wake (Fig. 2a and Fig. 2b). It appears some differences in the depth of the scour at $z = 0.4d$ and $z = 0.6d$ that can be attributed to the comparison on the first minutes of the phenomenon.

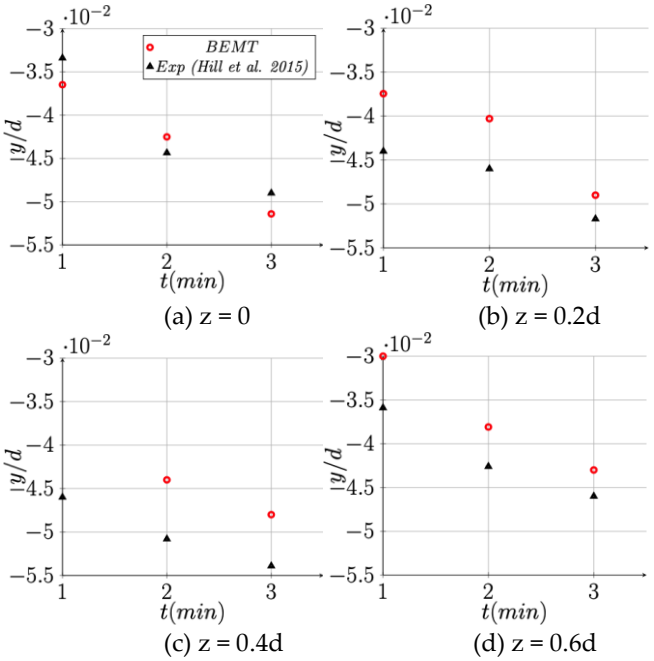

Fig. 2. Comparison of computed time series of bed elevation relative to the initial flat bed at *0.1d* downstream from the rotor and at (a) $z = 0$, (b) $z = 0.2d$, (c) $z = 0.4d$ and (d) $z = 0.6d$ (turbine is located at $z = 0$ in the spanwise direction): measurements by Hill et al. [1] (triangle); multiphase Euler-Euler with BEM (red circle)

III. TWO-TURBINES' CONFIGURATIONS

In this section, we consider the case of two turbines in tandem configuration over a sediment bed. Four different configurations are carried out in this section, for which the interaction of two axial hydrokinetic turbines, T1 and T2, are simulated in each configuration. The turbines are placed one behind the other axially in the computational channel. A layer of sand is spread out uniformly on the bottom of the channel below the turbines.

The disc of the first turbine T1, is placed at 1.51 m downstream the inlet, thus the one that represents the second turbine T2 is located at a distance d_i downstream from the first turbine. The axial distance inter-turbine d_i is the only parameter that differs between the configurations. It is defined as $d_1 = 4d$ for configuration A1, $d_2 = 7d$ for configuration A2, $d_3 = 10d$ for configuration A3 and $d_4 = 13d$ for configuration A4 (Fig. 3), where d is the diameter of

each turbine. The dimensions of the channel are *4m*0.35m*1m*. The turbine diameter is *d=0.08m*. The velocity ratio is *TSR = 2.1*, and *TI = 3%*. The bulk inlet velocity is *0.8 m/s*. The sediment volume fraction of the sand bed is *0.61* and its thickness is *0.05m* with a particle diameter d_s*=0.25 mm*. The physical parameters used in the case are the same as in previous case. As in the previous cases, the blades are modelled using 23 discrete NACA 63418 elements among their span. The fluid turbulence model k − ϵ has been used for both configurations and a time step of *0.001s* is imposed to approach the convergence. The mesh is created using blockMesh, it is configured as 60 million hexahedral mesh.

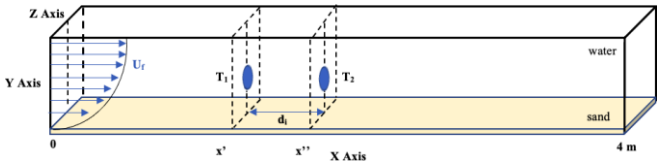

Fig. 3. Initial state of domain, position of the turbines (T1 and T2), logarithmic profile of the fluid velocity at inlet, the sheet layer of sands on the bottom (yellow color); d_i is the inter-turbines distance.

The bottom boundary used a smooth wall no slip condition and employed wall functions for the near wall flow. This allowed boundary layers to develop naturally along the tunnel test section. Within the OpenFOAM framework, for the TKE (Turbulent Kinetic Energy), a small fixed value can be used so as the kqRWallFunction that acts similarly as a Neumann boundary condition. At the outlet, zero-gradient conditions, are specified for all quantities, except for the reduce pressure p for which a uniform Dirichlet condition is imposed. At the top surface of the computational domain, Neumann conditions are applied for k and ϵ and for the three components of the velocity. Consequently, it cannot handle situations where the free surface is deformed near the structure. At the side, symmetry planes conditions are used. In inlet, the velocity is set to the logarithmic profile with the distance to the wall y, where u^* is the bed friction velocity, $\kappa = 0.41$ is the von Karman constant, and $k_s = 2.5ds$ is the Nikuradse roughness length in order to account for the bed roughness. This profile is set also as initial condition. Concerning the value of u_*, it is chosen to be *0.0369 m/s* greater than the critical value, $u^*_{cr} = 0.0342$ *m/s*. This latter is determined regarding the critical Shields parameter of the chosen sediment $\theta_{cr} = 0.043$, this corresponds therefore to a critical shear stress value of *0.1738 Pa*. In outlet, the hydrostatic pressure is fixed. At the top, a slip condition is imposed. The real bottom is considered as impermeable.

IV. RESULTS

A. Wake characterization

Fig. 4 presents axial velocity maps around the two interacting turbines. The wake behind the downstream turbine is altered by the influence of the upstream turbine. The downstream velocity deficit still remains contained in an axial strip, which is slightly larger than the one behind a single turbine. The wake also seems to recover slightly faster in terms of velocity deficit. The degradation of the axial velocity profiles is significant until 2d downstream the turbines. The velocity profiles under the first turbine (T1) are similar for all the inter-distances configurations, since the upstream velocities of (T1) are equal, however those under the second turbine (T2) are different between the configurations (Fig. 5).

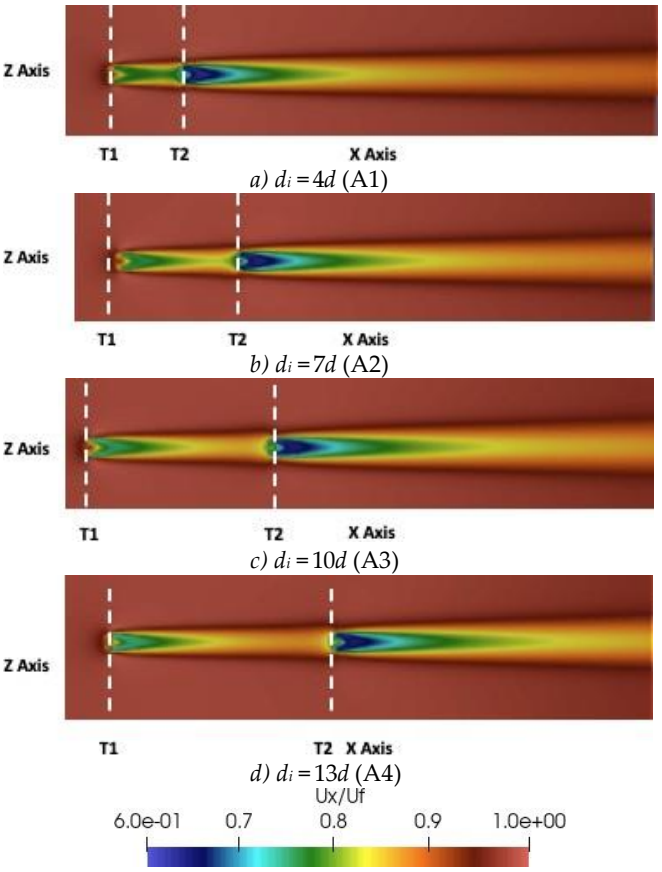

Fig. 4. Spatial evolution of bed elevation with the presence of two turbines apart with different di for configurations A1 (a), A2 (b), A3 (c) and A4 (d).

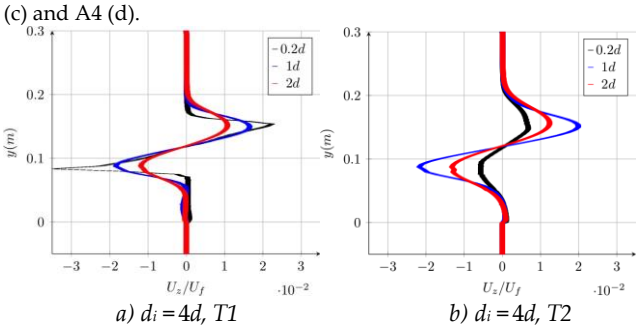

a) $d_i = 4d$, T1 b) $d_i = 4d$, T2

Fig. 5. Vertical profiles of velocity, normalized by the mean velocity of the fluid U_f upstream the turbines T1 and T2 for all configurations, at *0.2d* (black), *1d* (blue) and *2d* (red).

Indeed, depending on the inter-device distance, the flow at the location of the downstream turbine may not be homogeneous and may suffer as well from a velocity deficit as compared to the upstream velocity of the first turbine. As the inter-distance increases, as the upstream velocity value of the downstream turbine increases, then

the tangential velocities behind the upstream turbine are more important (fig. 5).

B. Turbines-sediments interaction

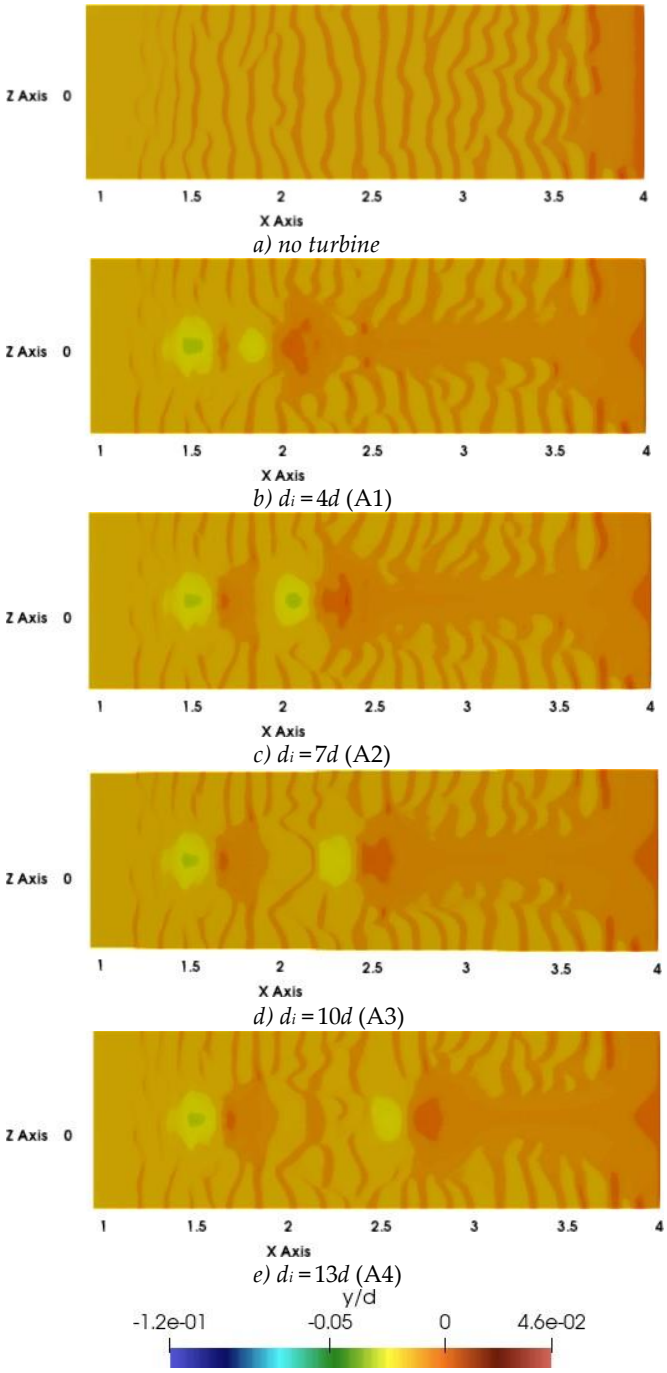

Fig. 6. Normalized elevations of the bottom (y/d) with and without the turbines; (a) baseline case, d_i = 4d, (c) d_i = 7d, (d) d_i = 10d and (e) d_i = 13d at 60 s.

Fig. 6 shows the modifications of the sediment bed due to the presence of the two turbines T1 and T2 for configurations A1, A2, A3 and A4 (Fig. 6b, 6c, 6d and 6e respectively). The bed form without the turbines is dominated by the sand ripples which are not homogeneous due to the canal walls effect (Fig. 6a).

The scour depth near the first turbine is almost the same for the four configurations, but we distinguish the difference of the scouring near the second turbine, since the position of the second turbine is widely different among the configurations (mainly in configuration A2, Fig. 6c). Thus, several changes in bed morphology have been found in the zone limited by the two turbines T1 and T2 between the configurations. The more the distance between turbines d_i increases, the more the bed is evolved. When $d_i = 4d$, T2 is close enough to T1 (Fig. 4a), so that the upstream velocity of T2 is the lowest compared to the ones of other configurations, this makes the flow less accelerated around the disk compared to other configurations, therefore it provides a less scouring under the second turbine.

Figures 7 and 8 present the spatial evolution of the normalized elevation of the bottom in two cross sections *0d* and *2d* downstream of the turbines at *t=60s*. The base line without turbine is located at *y/d=-1.5* (not represented here). Under T1 and T2 the erosion is significant. The scour reaches a depth of *0.03d* at *0d* (Fig. 7a and 8a). The presence of the turbine accelerates the flow around the disc, thus increases the shear stress and enhances the capability of the flow to erode the sediments. It forms a scour and leads subsequently to a varied morphology downstream the turbine.

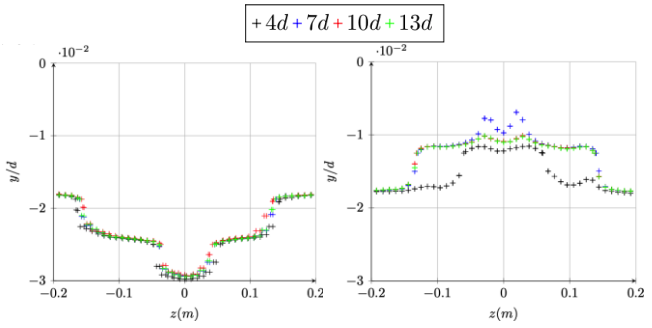

a) $0d, T_1$ b) $2d, T_1$

Fig. 7: Spatial evolution of the bed elevation at t = 60 s with the turbine at the cross sections of the T1 turbine's position (a); at the cross sections2d downstream T1.

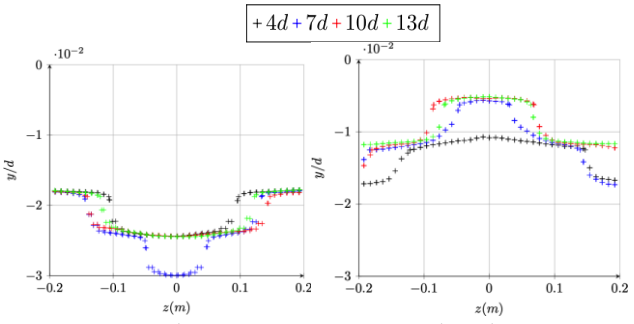

a) $0d, T_2$ b) $2d, T_2$

Fig. 8: Spatial evolution of the bed elevation at t = 60 s with the turbine at the cross sections of the T2 turbine's position (a); at the cross sections 2d downstream T2.

The turbine represented by an actuator BEM model induces a thrust force and a tangential force, these produce a reduction of the axial velocity in the turbine's wake and an increase of the tangential velocity which produces a swirl close to the turbine. This effect has been illustrated in Fig. 5, where the vertical profiles of z-component of the fluid velocity shows the impact of the turbine in the vertical axis across the turbine and in the wake.

The swirl and the induced hight vorticity close to the bottom produced by the turbine's rotation is largely reduced *2d* downstream the both turbines. This implies a reduction of the bed erosion. Moreover, at *2d*, a phenomenon of deposition occurs downstream of the turbines (Fig. 7b, 8b) since the bed elevation is greater than the baseline bed of *-1.5*. It can be observed large differences on the bottom elevation at the locations of turbines T1 and T2 (Fig. 7a and 8a). The reduction of the velocity in the wake of the turbine T2 produces less erosion under turbine T2. This indicate that the erosion under the turbine is a combination of the axial velocity and the swirl due to the turbine's rotation. 2d after the turbines (Fig. 7b and 8b) one observes a larger deposition downstream of T2 regarding T2. This is also in relation with the reduction of velocity in the wake of turbine T2 which favours the settling effect in this area.

The evolution of the bed morphology along the axial direction with and without the turbines for all configurations are provided in Fig. 9. The bed morphology maintains a cyclic ripples form in the baseline case all along the axis. When the turbines are activated, a scouring effect is observed at the location of the turbines and a deposition *2.5d* downstream of a turbine. When the two turbines are too close from each other, the respective effects of the turbines on bed morphology interact. The scour generated below the first turbine is the same for all configurations but after $X = 2d$ the evolution of the bed is widely different between the configurations. This is observed also for the second turbine.

Interactions are observed on the bed morphology on the case A1 and A2. The interactions are reduced for the two other cases, Thus the bed morphology downstream of the second turbine seem moved by *3d* downstream. Close downstream of the turbines no ripples are observed. But it reappears *6d* after the first turbine as in case A4. Downstream of the second turbine no ripples are observed. The further the second turbine is from the first, the more some ripples are lightly generated between the two turbines, similar to the baseline case. As in the case A4 *(13d)*, there is an attempt to produce a ripple especially at *8d* downstream the first turbine. This means that the flow at *8d* begins to recover (Fig. 9e) and the impact of the first turbine is less effective at this position in term of bed evolution, otherwise this ripple starts to disappear gradually from $X = 9d$ due to the intervention of the impact of the second turbine. The common point between all the configurations is that the bed is established beyond a distance *4d* downstream the second turbine, and maintains a constant elevation of *0.11d* equal to the pic of the ripples in baseline case. Those results show clearly the impact of the combination of two turbines on the bed morphology.

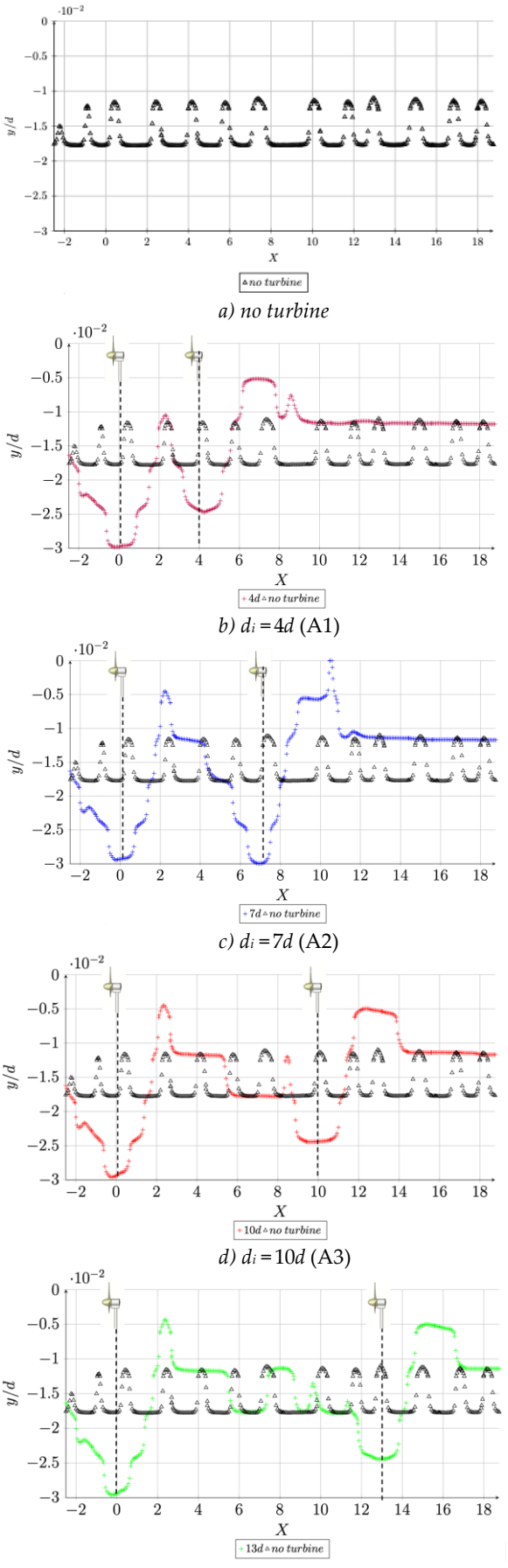

a) no turbine

b) $d_i = 4d$ (A1)

c) $d_i = 7d$ (A2)

d) $d_i = 10d$ (A3)

e) $d_i = 13d$ (A4)

Fig. 9. Normalized elevations of the bottom (y/d) with and without the turbines; (a) baseline case, $d_i = 4d$, (c) $d_i = 7d$, (d) $d_i = 10d$ and (e) $d_i = 13d$ at *60 s*.

V. CONCLUSIONS

In this work we couple a 3D Euler multi-phase model CFD approach to a BEMT model of an axial-flow three-bladed hydrokinetic turbine to study the interactions between the turbine and sediment transport of sandy bed.

A validation of the different part of the model has been succinctly described. Then a study of the combine effects of two turbines in tandem configuration on the sand bed morphology is performed with several distance between them. The wake distribution behind the second turbine is altered by the wake of the upstream turbine, and it is characterized depending on how far it is from the first turbine. Some points are listed hereafter:

- A scour is occurred below each turbine for all configurations, and a deposition is generated behind the turbines regarding the baseline results. The scour is more important under the first turbine.
- The bed under the second turbine evolves differently between the configurations, in term of erosion below the turbine and deposition downstream it.
- Results highlight how the interactions between turbines and channel morphology are coupled, and how the presence of single or multiple turbines can influence the local and far-field sediment transport characteristics.
- The further the second turbine is located away from the upstream turbine, the more the impact of this latter decreases on the wake distribution of the second, hence the impact of the turbines interaction on the sediment transport is less significant between their locations.

The case A2 ($d_i = 7d$) seems different from the others with a scour at the location of the second turbine as hight as the one at the first turbine. It needs more study to examine the reality of this singularity. So, a sensitivity of inter-distance values around $7d$ should be done in the future.

ACKNOWLEDGEMENT

The authors acknowledge the CRIANN (Centre Régional Informatique et d'Application Numériques de Normandie) co-financed by the Normandy Region, the French State and the European Union, for the access to the Computation means and to the Manche Country Council for their founding.

REFERENCES

[1] Hill C., Musa M., Guala M., "Interaction between instream axial flow hydrokinetic turbines and uni-directional flow bedforms", Renewable Energy, Vol. 86, pp. 409-421, 2015. Available: https://doi.org/10.1016/j.renene.2015.08.019

[2] Musa M., Hill C. and Guala M., "Interaction between hydrokinetic turbine wakes and sediment dynamics: array performance and geomorphic effects under different siting strategies and sediment transport conditions", Renewable Energy, Vol. 138, pp. 738-753, 2019. Available: http://doi.org/10.1016/j.renene.2019.02.009

[3] Cheng Z., Hsu T.-J., Calantoni J., "SedFoam: A multi-dimensional Eulerian two-phase model for sediment transport and its application to momentary bed failure". Coastal Engineering, Vol. 119, pp. 32-50, 2017. Available: https://doi.org/10.1016/j.coastaleng.2016.08.007

[4] Khaled F., Guillou S., Méar Y. and Hadri F., "Impact of Blockage Ratio on the Transport of Sediments in the presence of Hydrokinetic Turbine: Numerical Modelling of the Interaction Sediments-Turbine", International Journal of Sediment Research, Vol. 36, pp. 696-710, 2021. Available: http://doi.org/10.1016/j.ijsrc.2021.02.003.

[5] Chauchat J., Cheng Z., Nagel T., Bonamy C. and Hsu T. -J., "SedFoam-2.0: a 3-D two-phase flow numerical model for sediment transport", Journal of Geosci. Model Dev., Vol. 10, pp. 4367–4392, 2017. Available: http://doi.org/10.5194/gmd-10-4367-2017.

[6] Hsu T-J, Jenkins J. and Liu P., "On two-phase sediment transport: Sheet flow of massive particles". Proceedings of The Royal Society A: Mathematical, Physical and Engineering Sciences, Vol. 460, pp. 2223-2250, 2004. Available: http://doi.org/10.1098/rspa.2003.1273

[7] Chauchat J., and Guillou S., "On turbulence closures for two-phase sediment-laden flow models", J. Geophys. Res., Vol. 113, C11017, 2008. Available: https://doi.org/10.1029/2007JC004708

[8] Mycek P., Gaurier B., Germain G., Pinon G., Rivoalen E., "Experimental study of the turbulence intensity effects on marine current turbines behaviour", Part I: One single turbine. Renewable Energy, Vol. 66, pp. 729-746, 2014. Available: https://doi.org/10.1016/j.renene.2013.12.036

[9] Chauchat, J., and M. Médale, "A three-dimensional numerical model for dense granular flows based on the rheology", Journal of Computational Physics, Vol. 256(0), pp. 696 – 712, 2014. Available: http://doi.org/10.1016/j.jcp.2013.09.004.

[10] Hsu T.-J., Jenkins J. T. and Liu P. L.-F (2003), On two-phase sediment transport: Dilute flow, J. Geophys. Res., Vol. 108, N° C3, 3057. Available: http://doi.org/10.1029/2001JC001276.

[11] Lun C., Kinetic theory for granular flow of dense, slightly inelastic, slightly rough spheres, j. Fluid Mech., Vol. 233, pp. 539–559, 1991. Available: https://doi.org/10.1017/S0022112091000599